

Atomic Layer Epitaxy of Copper

Growth and Selectivity in the Cu(II)-2,2,6,6-tetramethyl-3,5-heptanedionate/H₂ Process

Per Mårtensson and Jan-Otto Carlsson

Department of Inorganic Chemistry, The Ångström Laboratory, S-75121 Uppsala, Sweden

ABSTRACT

The deposition of copper by means of atomic layer epitaxy is reported. Using Cu(II)-2,2,6,6-tetramethyl-3,5-heptanedionate as the precursor, pure and specular copper films were deposited at deposition temperatures below 200°C. This is more than 150°C lower than in previous reports for the same precursor where chemical vapor deposition has been employed. The process was self-limited in the temperature range 190 to 260°C. Area-selective deposition was achieved on platinum seeded substrates vs. unseeded glass slides or oxidized metal surfaces in the temperature range 175 to 300°C. At higher temperatures, the selectivity was lost, and nucleation was independent of substrate material because of a thermal decomposition of the precursor.

Introduction

It is expected that copper will replace aluminum and aluminum-based alloys as interconnect material in future advanced ultralarge scale integration (ULSI).¹ However, the lack of a suitable low-temperature route for copper deposition, the difficulty of etching the material, and the reactivity of copper with other components of the device are problems which have to be solved before this can become a reality.

The use of the copper(I) β -ketonates as precursors in chemical vapor deposition (CVD) has made copper deposition at temperatures below 200°C possible²⁻⁷ while the use of the copper(II) β -diketonates typically requires higher processing temperatures.⁸⁻¹¹ To prevent the reaction of copper with other components of the device, diffusion barriers are a requirement even when low-temperature processes are utilized. This barrier should also promote adhesion of copper as this is known to be poor on many of the materials used in integrated circuits (ICs).¹² Moreover, in order to reduce the number of process steps the barrier material should provide conditions for area-selective deposition.

Selective deposition of copper on metals vs. insulators and dielectric materials has been reported previously for CVD films prepared from metallorganic precursors.^{5,7,13,14} Among the copper(II) β -diketonates, i.e., the precursors of interest in atomic layer epitaxy (ALE), copper(II) 1,1,1,5,5,5-hexafluoro-2,4-pentanedionate, Cu(hfac)₂, has been the most extensively studied. (The reason that Cu(I) β -ketonates cannot be used in ALE is that they undergo a disproportionation on the substrate surface, resulting in a loss of the self-limitation of the process.) It has also been reported that copper can be deposited selectively on metals using this precursor.^{8,15-17} As Cu(hfac)₂ readily absorbs water and often exists as the hydrated form, studies have been carried out to clarify the influence of added water to the reaction gas mixture. The results of these studies have, however, been somewhat contradictory. While some authors have reported a loss of selectivity upon water addition, others have found that selectivity is not affected.¹⁸ In this context, Cu(II)-2,2,6,6-tetramethyl-3,5-heptanedionate, Cu(thd)₂, is interesting due to the fact that the very bulky ligands prevent the molecule from absorbing water, and Cu(thd)₂ is therefore stable for long periods of time even in an ambient atmosphere. As far as the authors know the selective deposition of copper, using this precursor, has not previously been reported.

ALE, introduced by Suntola and co-workers in 1977,¹⁹ is a technique which has proven to be well suited for the deposition of high quality thin films over large substrate areas.²⁰ A variety of materials have been fabricated by ALE, and, especially the II-VI^{21,22} and III-V compounds,^{23,24} as well as many of the transition metal oxides,²⁵ have earned great attention.

Thanks to its excellent throwing power, ALE can be used for thin film deposition on very complicated shaped

substrates and even on powders. This is a unique feature of the ALE process and can be exemplified by the deposition of mixed oxides on high surface area powders.²⁶

ALE is also suitable for in situ studies of the deposition process due to the separation of the reaction steps. For instance, reports have been published on the use of quartz crystal microbalance (QCM),²⁷ incremental dielectric reflection, IDR,²⁸ reflection high-energy electron diffraction (RHEED),^{29,30} and low energy ion scattering (LEIS)³¹ for monitoring of the adsorption and reaction of the precursor molecules on the substrate surface.

Finally, typical process temperatures are lower in ALE than in corresponding CVD processes. An important example in this context is the deposition of TiN. The TiCl₄/NH₃ process typically demands deposition temperatures close to 700°C to get chlorine-free films with CVD³² while this has been achieved already at 500°C³³ by ALE.

In this paper we report on area-selective and nonselective copper deposition by ALE using Cu(thd)₂ as the copper precursor and H₂ as the reducing agent.

Experimental

Thin copper films were deposited on 25 × 25 mm soda-lime glass substrates with a seed layer consisting of a mixture of platinum and palladium. This seed layer was produced by sputtering and was typically only a few angstroms thick. Prior to the sputtering, the glass slides were washed in ethanol and boiling acetone and finally blown dry in a nitrogen flow. The patterned substrates were prepared by masking a glass substrate with either ordinary adhesive tape or by a photoresist prior to the sputtering of the seed layer. For selectivity studies, tantalum, iron, titanium nitride, nickel, and indium-tin oxide (ITO) were also used as substrates. These substrates are all metallic but also known to form surface oxides upon exposure to air. They were, in spite of this, used without any hydrogen preclean as the effects of such a treatment could not be studied without exposing the sample to the ambient atmosphere. All substrates were blown clean with nitrogen or air prior to the experiment.

The experiments were carried out in a three-zone hot wall ALE reactor built at the department (Fig. 1). Cu(thd)₂, (Strem Chemicals, claimed purity 99%) was used as the precursor without further purification and hydrogen (AGA, claimed purity 99.9995%) was used as the reducing

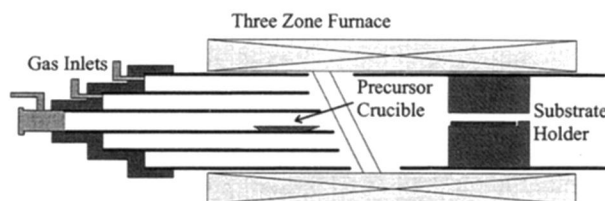


Fig. 1. The ALE setup.

agent. Nitrogen (AGA, claimed purity 99.9999%) was used as the carrier gas. The experiments were performed at a total pressure of 5 to 10 Torr and the deposition temperature was varied between 150 and 350°C. The evaporation temperature of the precursor was always 120°C.

The elemental composition of the films was determined by X-ray photoelectron spectroscopy (XPS), using a Perkin Elmer PHI 5500 multianalysis system. Hydrogen concentration was determined by nuclear reaction analysis (NRA) at the tandem accelerator laboratory in Uppsala. A ^{15}N beam was used to excite the 6.4 MeV resonance of the $^1\text{H}(^{15}\text{N}, \alpha\gamma)^{12}\text{C}$ reaction. Phase identification was performed by X-ray diffraction (XRD, Siemens D-5000 diffractometer with $\text{Cu K}\alpha$ radiation) with the grazing incidence method. The angle of incidence was 1° and the scan range was $10^\circ < 2\theta < 80^\circ$.

Film thickness was measured by X-ray fluorescence spectrometry using a Philips PW 1410 X-ray fluorescence spectrometer. This method gives an average density of atoms over an area of approximately 19 mm^2 rather than a direct value of the film thickness. The film thickness reported here have been obtained by comparing the signal from the sample with a previously recorded calibration curve. This curve was obtained from standards (copper sputtered on glass) with well-known thicknesses. In these measurements the density of the deposited films was assumed to be the same as for the standards.

The morphology of the copper film was studied by means of atomic force microscopy (AFM, Topometrix Explorer) as well as by scanning electron microscopy (SEM), using a JEOL JSM 840 scanning electron microscope.

Film resistivity was measured by a standard four-point probe method and the adhesion was evaluated by means of the Scotch[®]tape test.

Results

Film properties.—The deposited copper films were specular and showed strong adhesion to the substrate. X-ray diffraction found them to be polycrystalline and possessing no preferential growth direction (Fig. 2). The intensity ratio of the diffraction peaks corresponds well to that of a bulk sample.³⁴ The use of a seed layer thicker than approximately 60 Å led to the appearance of new peaks at just slightly lower 2θ values than the corresponding copper peaks. This was attributed to the formation of Cu_3Pt . This phase is, like copper, cubic with an a axis only slightly longer than that of copper (2.4%).³⁵

The polycrystalline nature of the copper films was verified in SEM and AFM studies which also showed that the size of the individual grains was in the range 0.1 to 0.3 μm and depended on the film thickness (Fig. 3). The size of the grains did not vary with the deposition temperature in the ALE temperature window (190 to 260°C) but increased with increasing film thickness. The surface roughness was only dependent on film thickness and not on the deposi-

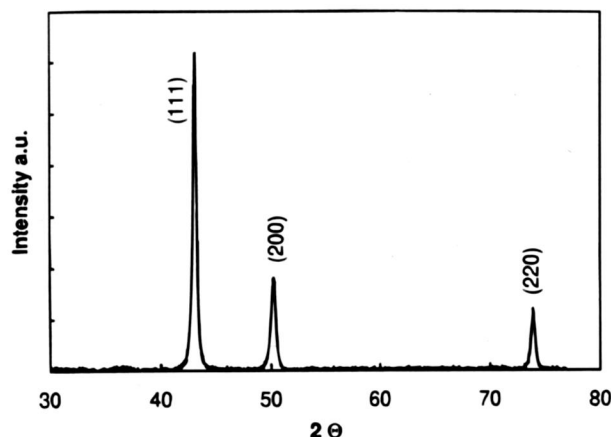


Fig. 2. X-ray diffraction pattern of copper deposited at 250°C.

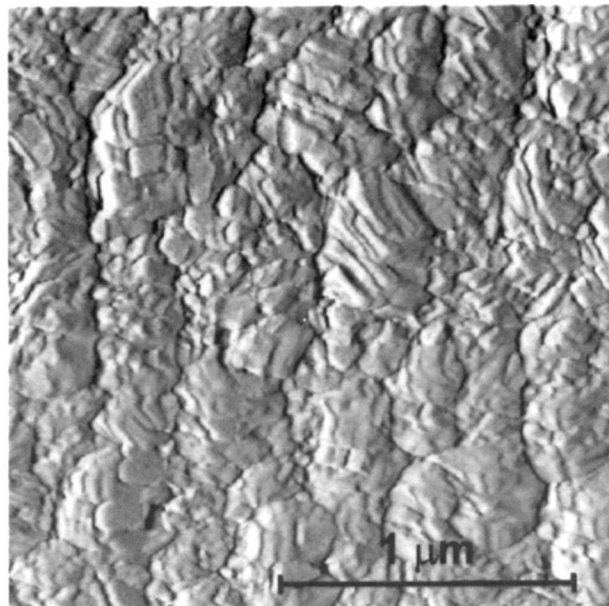


Fig. 3. AFM micrograph showing the morphology of copper deposited at 230°C.

tion temperature in this temperature window and the films were also homogenous over the whole substrate area. A minimum in surface roughness was achieved after approximately 200 cycles, i.e., after 70 to 80 Å of copper had been deposited. A plausible explanation to this behavior is that the nucleation of the film did not occur homogeneously across the substrate surface but rather as islands. Upon coalescence of the individual nuclei, the roughness of the film reaches a minimum. However, with increasing film thickness, the size of the individual grains increases, as does the roughness.

Above 300°C, the morphology started to change and the copper films were no longer smooth and mirrorlike but became increasingly dull as the temperature increased. The thickness profile of the deposit across the substrate surface showed a similar temperature dependence. At lower temperatures, the copper was homogeneously deposited across the substrate surface, but as the temperature in the deposition zone increased above 300°C, a thickness profile was developed with the thickest film at the leading edge of the substrate.

According to the XPS analysis, the copper films were very pure. After removal of surface contaminants by argon sputtering, only traces of carbon and oxygen were found. However, in samples which had been deposited on substrates with a seed layer thicker than approximately 60 Å, platinum and palladium could also be detected. The concentration of oxygen was very low in all samples, while the carbon concentration varied between samples deposited at similar conditions but with different cooling procedures. Samples which had been allowed to cool under a hydrogen atmosphere contained a lower concentration of carbon than could be detected by XPS. However, in samples which had been cooled under nitrogen flow the carbon concentration after 30 s of sputtering, varied from 12 to 14 atom % in samples deposited below 300°C to 19 atom % for samples deposited at 350°C. From the NRA measurements the hydrogen concentration in the copper films was below 3 atom %.

The resistivity of the films was high. A 600 Å thick film had a resistivity of approximately $8\text{ }\mu\Omega\text{ cm}$, which is a factor of five higher than that of bulk copper, and it increased with decreasing film thickness (Table I). This was, however, not unexpected, as thin films are known to have higher resistivity than bulk materials. Since the AFM studies showed that the films consist of well-connected grains and the XPS measurements showed that the films were also free from carbon and oxygen contamination, the high

Table I. Resistivity for copper films of various thickness.

| Film thickness (Å) | Resistivity ($\mu\Omega$ cm) |
|--------------------|-------------------------------|
| 600 | 8.1 |
| 540 | 12.5 |
| 453 | 30.3 |
| 409 | 41.2 |

resistivity might be attributed to the film thickness rather than to a poor quality of the films. This conclusion is also supported by the findings made by Rycroft and Evans.³⁶ They studied the resistivity of copper films as a function of film thickness and showed that even though the film was continuous the resistivity was still far from bulk values.

Selectivity.—Selective deposition on the seeded substrate areas vs. the unseeded occurred at temperatures up to approximately 300°C, and the interface between the seeded and unseeded regions was sharp and distinct (Fig. 4). However, even though a completely covering film could not be observed on the unseeded areas at 350°C, a number of small grains appeared already above approximately 300°C, i.e., the selectivity temperature is below 300°C. To further investigate the mechanism of the selectivity process, tantalum, iron, nickel, titanium nitride, and ITO were used as substrates. We found that even though we used the optimum experimental growth parameters, no film growth could be observed on any of these substrates.

Deposition mechanism and kinetics.—For an introduction to ALE and the various process steps used in the discussion that follows, see Ref. 37.

The process was self-limited in the temperature range 190 to 260°C (Fig. 5). The maximum deposition rate in this range was reached after a precursor pulse duration of 4 s and was approximately 0.17 monolayer/cycle (Fig. 6). In the experiments presented in Fig. 5, the duration of the precursor pulse was only 2 s. This explains the lower deposition rate.

At temperatures below the self-limited regime, the deposition rate decreased abruptly, and at 150°C, almost no growth could be observed. Upon increasing the partial pressure of hydrogen as well as the duration of the hydrogen pulse at 175°C, an increase in the deposition rate (in Å/cycle) was observed (Fig. 7). Finally, because of a ther-

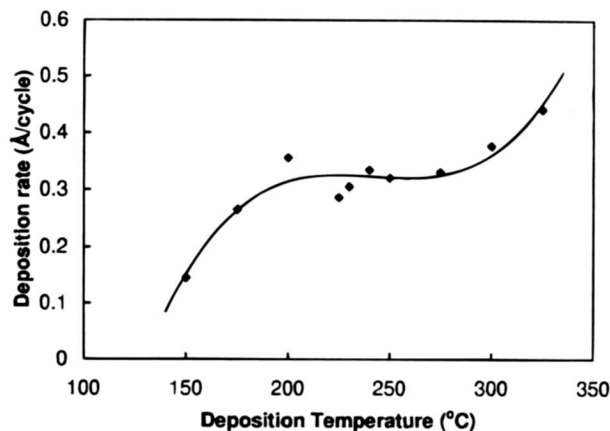


Fig. 5. Deposition rate as a function of the deposition temperature for copper deposited on platinum seeded glass substrates.

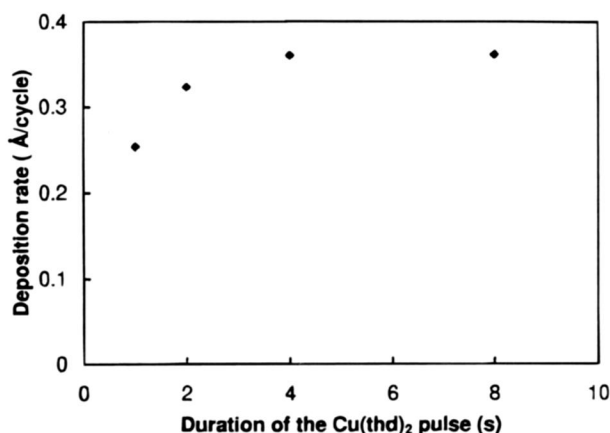


Fig. 6. Effect of duration of the $\text{Cu}(\text{thd})_2$ pulse on the copper deposition rate at 230°C.

mal decomposition of the precursor, the deposition rate, as well as the amount of carbon contamination, increased when the temperature in the deposition zone was increased above the ALE temperature window.

Discussion

In the following, the deposition mechanisms are discussed on the basis of the observations presented above. The findings in the high- and low-temperature regimes as well as in the ALE temperature window are discussed separately.

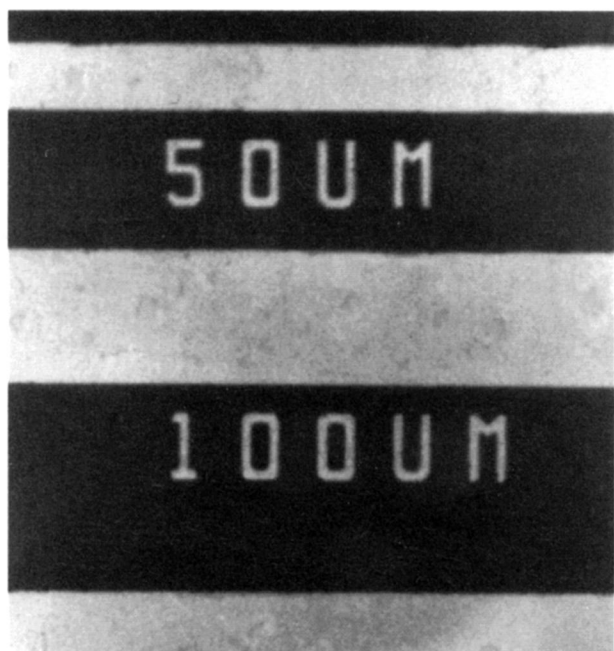


Fig. 4. An overview image of copper deposited on a patterned substrate.

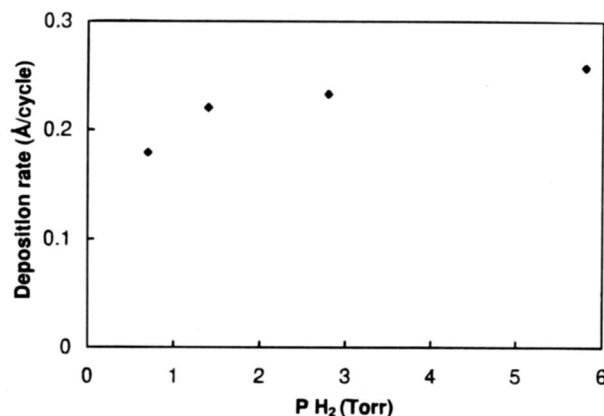


Fig. 7. Effect of hydrogen partial pressure on the deposition rate for copper deposited at 175°C.

Low-temperature regime (below 180°C).—The decreased deposition rate at lower temperatures can be explained by either reduced adsorption or by slow kinetics in the reduction step. The results found on varying the reduction parameters, i.e., the hydrogen partial pressure and the duration of the hydrogen pulse, leads to the conclusion that it is the slow kinetics in the reduction step that causes the decreased deposition rate. Whether the rate determining step is the dissociation of the hydrogen molecule or the reaction between the adsorbed ligands and the hydrogen, cannot be verified by these experiments, and is not further discussed here.

ALE temperature window (190 to 260°C).—In this regime, the process was self-limited, and copper could be area-selectively deposited on platinum seeded glass vs. all other substrate materials used in this study. The self-limitation of the process shows that the precursor is stable enough to avoid decomposition in this temperature range but the fact that film growth occurs shows that the kinetics is fast enough to allow film growth at an acceptable rate on metallic areas.

Even though the self-limitation can be explained in terms of kinetics, the origin of the selectivity is more difficult to understand. There are, however, two clearly distinguishable processes that might account for this. (i) The $\text{Cu}(\text{thd})_2$ molecule cannot adsorb properly due to lack of available adsorption sites. (ii) The molecule adsorbs but the ligands cannot be removed during the reduction step and the process terminates after that one monolayer of $\text{Cu}(\text{thd})_2$ has been adsorbed.

As the metallic substrates used in this study (Ta, Fe, TiN, Ni, and ITO) are known to form surface oxides upon exposure to air, and surface oxides are normally terminated by hydroxyl groups, the first of these two possibilities can be ruled out from the findings by Haukka et al.²⁶ They have shown that molecules of the type $\text{M}^{n+}(\text{thd})_n$ adsorb readily on hydroxyl-terminated oxide surfaces.

The other possibility, i.e., that the ligands cannot be removed during the reduction step, is strongly supported by Cohen et al.³⁸ They suggest that copper deposition from $\text{Cu}(\text{hfac})_2$, a compound in the same family as $\text{Cu}(\text{thd})_2$, occurs via the dissociation of the $\text{Cu}(\text{hfac})_2$ molecule on the surface of the substrate. During this step one or both of the ligands are lost as copper is partially reduced through electron transfer from the substrate. Finally, a reaction intermediate is formed as well as free hfac ligands which occupy adjacent adsorption sites. (The state of the $\text{Cu}(\text{hfac})_2$ molecule and the bonding between the ligands and the surface/copper atom was not unambiguously determined in the referred to investigation.) The hfac ligands can only be removed by the addition of an external reducing agent or as an intact $\text{Cu}(\text{hfac})_2$ molecule. No copper will be deposited if the latter process occurs and the use of an external reducing agent will therefore be needed for film growth. Moreover, Cohen et al. claim that for the initial activation of the process, i.e., the reduction of the copper atom and the loss of one (or perhaps both) of the ligands, “the presence of electron rich metallic substrates appears to be extremely important.” Our findings are in good agreement with this statement. Hence, the reason that copper cannot be deposited on insulators and oxidized metals by this process is that the electrons in the substrate are not available for the adsorbed precursor molecules, and this lack of “activation” terminates the process.

However, there remain at least two alternative explanations to why electrons cannot be transferred to the molecule. Either the electron transport is hindered by a thick and insulating surface oxide, or by a strong and localized $\text{O}_{\text{surface}}\text{-Cu}$ bond. From the deposition experiments where Ta, TiN, Fe, and Ni were used as substrates, no unambiguous conclusions could be found on the origin of the selectivity, because these substrates are all covered by a hydroxyl-terminated surface oxide of unknown thickness.

The fact that copper could not be deposited on ITO gave an interesting clue to the selectivity of this process. Because ITO is metallic, there are free electrons which are available for the activation of the $\text{Cu}(\text{thd})_2$ molecule during the adsorption step. (This was, according to Cohen et al.,³⁸ one of the main requirements for film growth when $\text{Cu}(\text{hfac})_2$ was used as precursor.) Furthermore, because ITO is an oxide, the surface atoms are not expected to be affected by exposure to air, and the surface conductivity should, thus, be close to that of the bulk material. Being an oxide, ITO is also assumed to be terminated by hydroxyl groups. It was assumed that if copper could be grown on ITO, the origin of the selectivity would be the availability of free electrons in the substrate, i.e., that the surface oxide on Ta, Fe, Ni, and TiN would be thick enough to be an effective insulator. However, if film growth did not occur on ITO, the main reason for the selectivity would, thus, be found in the bonding between the oxygen of the hydroxyl group and the copper atom.

From the fact that no growth was observed on ITO, comes the conclusion that the lack of film growth on oxides and oxidized metal surfaces is not caused by the presence of a surface oxide, but that the surface is hydroxyl terminated. This gives a strong $\text{O}_{\text{surface}}\text{-Cu}$ bond through which electrons cannot be transferred.

This conclusion is further supported by Haukka et al.²⁶ They suggest that upon adsorption of a $\text{M}^{n+}(\text{thd})_n$ molecule on a hydroxyl-terminated surface, the molecule dissociates and loses one or several, but never all its ligands. The dissociated ligands then form volatile $\text{H}(\text{thd})$ molecules through proton transfer from the OH-groups on the substrate surface to which the molecule binds. To remove the remaining ligands from the metal atom, Haukka et al. added air or water vapor for several hours with a subsequent increase in the temperature in the reaction chamber. This treatment left the surface in a state where the formed metal oxide surface was covered with -OH groups. However, the temperature used during this step, 450°C, is high enough to thermally decompose the ligands so that the reaction products are likely not only $\text{H}(\text{thd})$ molecules but also molecules with shorter hydrocarbon chains as well as CO_2 and H_2O . In the experiments presented in this paper, where a much lower deposition temperature is used, this decomposition does not occur at a significant rate, and the surface will remain occupied by precursor molecules.

The adsorption of $\text{Cu}(\text{thd})_2$ on hydroxyl terminated surfaces has also been studied by Sekine et al.^{39,40} Contrary to the findings by Haukka and co-workers, they suggest that the molecule is intact under adsorption and binds to two hydroxyl groups. These hydroxyl groups lose their hydrogen atoms which are then transferred to the same carbon atom as suggested by Haukka et al. (see Fig. 8). However, as their investigation was not complete, no unambiguous model for the bonding between the surface hydroxyl groups and the adsorbed molecule was proposed.

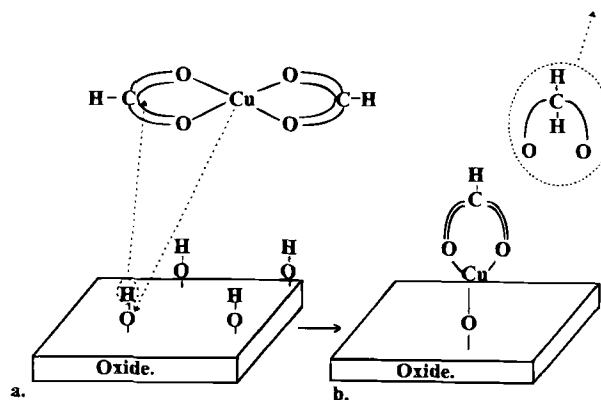


Fig. 8. Proposed reaction mechanism for the deposition of copper on hydroxyl-terminated surfaces.

Our conclusions are also supported by the findings by Becht et al.⁹ They found that copper could be grown on quartz substrates in the temperature range 350 to 750°C in a pure hydrogen atmosphere, whereas no film growth was observed at deposition temperatures below 350°C. Following the results in our experiments, their observations can be explained by a thermal decomposition of the precursor on the substrate surface at higher temperatures. At lower temperatures, however, the surface species are stable enough to avoid decomposition and, hence, film growth cannot occur.

High-temperature regime (above 275°C).—The increased deposition rate at higher processing temperatures can, as mentioned above, be explained by the thermal decomposition of the precursor during the adsorption step. The dissociation of the precursor and the subsequent desorption of the more or less decomposed ligands renders new adsorption sites and the self-limitation of the process is lost. As the ligands decompose, some carbon and oxygen are also incorporated into the growing film. The deposition rate in this process is dependent on the supply of precursor rather than the kinetics in the reduction step, and the ALE-type growth is replaced by continuous growth. As a consequence of this decomposition, a thickness profile of the deposit across the substrate surface is developed. The thickest film was found at the leading edge of the substrate and a thinner film at the far end, which was due to gas-phase depletion.

The selectivity of the process was also partially lost in this temperature regime. The coincidence of the loss of selectivity with the increase in contamination content makes it tempting to relate the two observations to the same process, i.e., to the thermal decomposition of the precursor on the substrate surface and a subsequent nucleation of copper.

These findings are also in accordance with those of Hanoka et al.⁴¹ who studied the stability of the Cu(thd)₂ molecule both in the gas phase above a heated substrate and on a substrate surface under CVD conditions. They found that Cu(thd)₂ is stable in the gas phase above a substrate heated to 500°C, but decomposes at higher temperatures. They reported later that the amount of carbon in a deposited film increased slowly above 300°C and more rapidly above 500°C.⁴² This was explained by the fact that the precursor decomposes only on the substrate surface at lower temperatures while the decomposition occurs also in the gas phase above 500°C.

Tobaly and Lanchec⁴³ observed that the Cu(thd)₂ molecule decomposes at 160°C under equilibrium conditions in a closed evacuated glass cell, although the specification from Strem states that the decomposition occurs at the boiling point, i.e., at 315°C, and that melting occurs at 198°C. This investigation has shown that decomposition is slow at temperatures below 300°C, explaining the low contamination content. At higher temperatures, the decomposition is faster and consequently the carbon contamination increases unless hydrogen is supplied during the cooling-down sequence.

Conclusions

Area-selective deposition of copper on platinum/palladium seeded substrates vs. unseeded glass and oxidized metal substrates at temperatures below approximately 300°C has been reported. The process was self-limited in the temperature range 190 to 260°C in which the maximum deposition rate was approximately 0.17 monolayers per cycle. The temperatures used in this study are 100 to 150°C lower than those previously reported for this precursor when CVD has been employed.

The underlying mechanisms for film growth and selectivity are complicated. It is concluded, however, that the main requirement for film growth at the low temperatures used in this process is that the molecule should be able to dissociate on the substrate surface. At substrate surfaces, where this dissociation cannot occur, i.e., on hydroxyl terminated oxides and oxidized metal surfaces, film growth

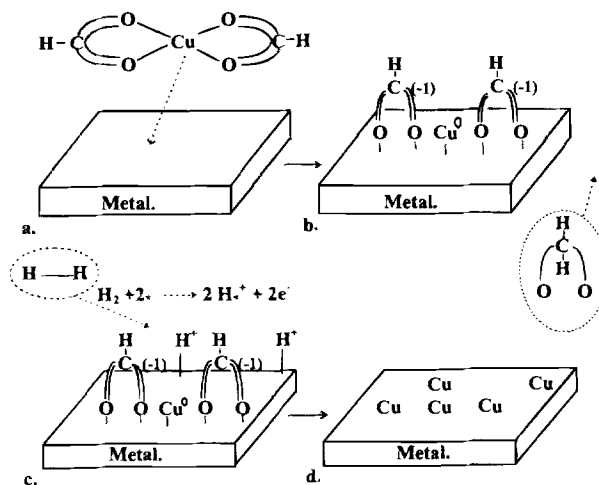


Fig. 9. Proposed reaction mechanism for the deposition of copper on pure metals.

is not observed. The proposed mechanisms, explaining the different reaction steps in copper deposition on different substrate materials, are summarized in Fig. 8 and 9. Upon adsorption of Cu(thd)₂ on a hydroxyl terminated surface, the copper atom replaces the hydrogen of the hydroxyl group, and a bond is formed between the copper and the oxygen atom. The hydrogen is transferred to one of the ligands (Fig. 8a), which is then removed as a volatile H(thd) molecule. The second ligand cannot be removed at the temperatures used in this study, and a blocking of the surface sites is obtained (Fig. 8b). The deposition process will then cease after the adsorption of one monolayer of Cu(thd)₂. At metal surfaces, however, (Fig. 9a-d) the dissociation of the Cu(thd)₂ molecule is more complete due to the electron transfer from the substrate to the adsorbed molecule. (The ligand-surface bonding presented in Fig. 9c and d should not be accepted as "true" but more as a schematic.) Upon hydrogen adsorption, electrons are supplied to the substrate and the ligands can be completely removed as H(thd) through reaction with the adsorbed hydrogen.

Acknowledgments

The authors are grateful to the Ångström Consortium and the Natural Science Research Council for financial support. L. Jonsson at the Department of Materials Science is acknowledged for providing the patterned substrates, and Dr. Björgvin Hjörvarsson is acknowledged for assistance with the nuclear reaction analysis measurements.

Manuscript submitted October 14, 1997; revised manuscript received April 8, 1998.

Uppsala University, assisted in meeting the publication costs of this article.

REFERENCES

1. S. P. Murarka, *Mater. Sci. Eng., R*, **19**, 87 (1997).
2. A. Jain, K.-M. Chi, T. T. Kodas, and M. J. Hampden-Smith, *J. Electrochem. Soc.*, **140**, 1434 (1993).
3. G. Braeckelmann, D. Manger, A. Burke, G. G. Peterson, A. E. Kaloyeros, C. Reidsema, T. R. Omstead, J. F. Loan, and J. J. Sullivan, *J. Vac. Sci. Technol. B*, **14**, 1828 (1996).
4. P. Doppelt and T. H. Baum, *Thin Solid Films*, **270**, 480 (1995).
5. J. B. Webb, D. Northcott, and I. Emesh, *Thin Solid Films*, **270**, 483 (1995).
6. E. S. Choi, S. K. Park, and H. H. Lee, *J. Electrochem. Soc.*, **143**, 624 (1996).
7. E.-C. Plappert, T. Stumm, H. van den Bergh, R. Hauert, and K.-H. Dahmen, *Chem. Vap. Deposit.*, **3**, 37 (1997).
8. N. Awaya and Y. Arita, *Jpn. J. Appl. Phys.*, **32**, 3915 (1993).
9. M. Becht, K.-H. Dahmen, F. Atamny, and A. Baiker, *Fresenius' J. Anal. Chem.*, **353**, 718 (1995).

10. M. B. Naik, W. N. Gill, R. H. Wentdorf, and R. R. Reeves, *Thin Solid Films*, **262**, 60 (1995).
11. J.-Y. Kim, P. J. Reucroft, and D.-K. Park, *Thin Solid Films*, **289**, 184 (1996).
12. S. P. Murarka and S. W. Hymes, *Crit. Rev. Solid State Mater. Sci.*, **20**, 87 (1995).
13. A. Jain, T. T. Kodas, R. Jairath, and M. J. Hampden-Smith, *J. Vac. Sci. Technol., B*, **11**, 2107 (1993).
14. H.-K. Shin, K.-M. Chi, M. J. Hampden-Smith, T. T. Kodas, J. D. Farr, and M. Paffet, *Adv. Mater.*, **3**, 246 (1991).
15. D.-H. Kim, R. H. Wentdorf, and W. N. Gill, *J. Vac. Sci. Technol. A*, **12**, 153 (1994).
16. N. Awaya, K. Ohno, and Y. Arita, *J. Electrochem. Soc.*, **142**, 3173 (1995).
17. B. Lecohier, B. Calpini, J.-M. Philippox, and H. Van den Bergh, *J. Appl. Phys.*, **72**, 2022 (1992).
18. See, e.g., G. L. Griffin and A. W. Maverick, in *The Chemistry of Metal CVD* T. T. Kodas and M. J. Hampden-Smith, Editors, Chap. 4, VCH, Weinheim (1994) and references therein.
19. T. Suntola and J. Antson, U.S. Pat. 4,058, 430 (1977).
20. T. Suntola, *Appl. Surf. Sci.*, **100/101**, 391 (1996).
21. P. Soinenen, E. Nykänen, L. Niinistö, and M. Leskelä, *Chem. Vap. Deposition*, **2**, 69 (1996).
22. T. Pakkanen (Chap. 2) and T. Yao (Chap. 5), in *Atomic Layer Epitaxy* T. Suntola and M. Simpson, Editors, Blackie, Glasgow (1990) and references therein.
23. J.-S. Lee, S. Iwai, H. Isshiki, T. Meguro, T. Sugano, and Y. Aoyagi, *Appl. Surf. Sci.*, **103**, 275 (1996).
24. K. Mukai, N. Ohtsuka, H. Shoji, and M. Sugawara, *Appl. Surf. Sci.*, **112**, 102 (1997).
25. L. Niinistö, M. Ritala, and M. Leskelä, *Mater. Sci. Eng. B*, **41**, 23 (1997).
26. S. Haukka, M. Lindblad, and T. Suntola, *Appl. Surf. Sci.*, **112**, 23 (1997).
27. J. Aarik, K. Kukli, A. Aidla, and L. Pung, *Appl. Surf. Sci.*, **103**, 331 (1996).
28. A. Rosental, P. Adamson, A. Gerst, H. Koppel, and A. Tarre, *Appl. Surf. Sci.*, **112**, 82 (1997).
29. J. M. Hartmann, G. Feuillet, M. Charleux, and H. Mariette, *J. Appl. Phys.*, **79**, 3035 (1996).
30. B. Y. Maa and P. D. Dapkus, *J. Electron. Mater.*, **19**, 289 (1990).
31. R. G. van Welzenis, R. A. M. Bink, and H. H. Brongersma, *Appl. Surf. Sci.*, **107**, 255 (1996).
32. J. B. Price, J. O. Borland, and S. Selbrede, *Thin Solid Films*, **236**, 311 (1993).
33. M. Ritala, M. Leskelä, E. Rauhala, and P. Haussalo, *J. Electrochem. Soc.*, **142**, 2731 (1995).
34. H. E. Swanson and E. Tatge, JCPDF card no. 4-836, Swarthmore, PA.
35. C. J. Humphreys, JCPDF card no. 35-1358, Swarthmore, PA.
36. I. M. Rycroft and B. L. Evans, *Thin Solid Films*, **290-291**, 283 (1996).
37. M. Leskelä and L. Niinistö, in *Atomic Layer Epitaxy*, T. Suntola and M. Simpson, Editors, Chap. 1, Blackie, Glasgow (1990) and references therein.
38. S. L. Cohen, M. Liehr, and S. Kasi, *Appl. Phys. Lett.*, **60**, 50 (1992).
39. R. Sekine and M. Kawai, *Appl. Phys. Lett.*, **56**, 1466 (1990).
40. R. Sekine, M. Kawai, T. Hikita, and T. Hanada, *Surf. Sci.*, **242**, 508 (1991).
41. K.-I. Hanoka, H. Ohnishi, H. Harima, and K. Tachibana, *Physica C*, **190**, 145 (1991).
42. K.-I. Hanoka, H. Ohnishi, and K. Tachibana, *Jpn. J. Appl. Phys.*, **32**, 4774 (1993).
43. P. Tobaly and G. Lanchec, *J. Chem. Thermodyn.*, **25**, 503 (1993).

Wet Chemical Etching for V-grooves into InP Substrates

J. Wang, D. A. Thompson, and J. G. Simmons

Center for Electrophotonic Materials and Devices and Department of Engineering Physics, McMaster University, Hamilton, Ontario L8S 4L7, Canada

ABSTRACT

A systematic study has been performed on the production of V-grooves in (100) InP substrates by wet chemical etching. The dissolution process and its dependence on etchant, etch mask, and its accuracy of alignment relative to the [011] or [0 $\bar{1}1$] directions has been analyzed. Consequently, the conditions necessary to achieve V-grooves having (111)A, (111)B, and (211)A sidewalls has been established.

Introduction

InP-based devices are playing important roles in optical telecommunication, microwave, high-speed digital, and analog applications; however, the technology is relatively immature compared to that of GaAs. Chemical etching is an essential step in device processing and needs to be well understood and controlled in order that features of well-defined geometry can be fabricated. Recently there has been interest in the possibility of producing quantum wire (QWR) lasers using epitaxial growth on V-groove etched substrates.¹⁻³ Here the morphology and geometry of groove profiles critically affects the final growth of quantum structures.

V-groove etching, as a specific example of preferential etching, is attributed to crystallographic structure: in particular, if the etching is not diffusion-controlled it depends on the configuration of surface atoms and the bond structure.⁴ It is those crystal planes with slowest etch rate that determine the etch profile. Most commonly, V-grooves etched into III-V semiconductors have (111)A, (111)B, or (211)A sidewalls.¹⁻³ Both wet chemical etching⁵⁻⁹ and dry chemical etching¹⁰⁻¹² can be used to make V-grooves. Until now almost all V-grooves used for QWR fabrication have

been obtained with wet chemical etching, which is simple, flexible, and less equipment demanding than dry etching. Recently PCl₃ gas has been used to etch InP in a molecular beam epitaxy (MBE) chamber, and channels containing (011), (111)A, and (111)B facets, and V-shape-like grooves, have been produced. However, a close examination of the sharpness of the groove bottom has not been reported.^{10,11}

Preferential wet etching of III-V compounds, including InP, has been studied for many years.^{13,14,16-22} However, little work has been reported on etching to produce sharp V-grooves with smooth sidewalls as required for QWR fabrication.^{5-9,15} Huo et al.⁶⁻⁸ studied groove profiles etched on InP using HCl-based solutions and Wang et al.⁹ reported the effect of native oxide on mask undercutting of V-grooves, but no detailed information has been provided on the sharpness or the profiles at the bottoms of the V-grooves. Recently, Kappelt and Bimberg¹⁵ reported (111)A V-grooves with sharp bottoms and smooth sidewalls using a three-step etching process. In this work we report on etching experiments using different etchants, and mask materials for grooves aligned [011] and [0 $\bar{1}1$], as well as having different degrees of mask misalignment relative to the [011] or [0 $\bar{1}1$] directions. Also, the etching processes and their dependence on surface orientation are analyzed. Based on